Particle-in-Cell Simulations of Relativistic Weibel-Mediated Shocks Propagating into Inhomogeneous Media

arXiv: 1907.08939

Sara Tomita and Yutaka Ohira
(Aoyama Gakuin University) **(University of Tokyo)**

ICRC2019, July 24 – August 1, 2019, Madison, USA

The origin of 10^{17}eV cosmic-rays (CRs)

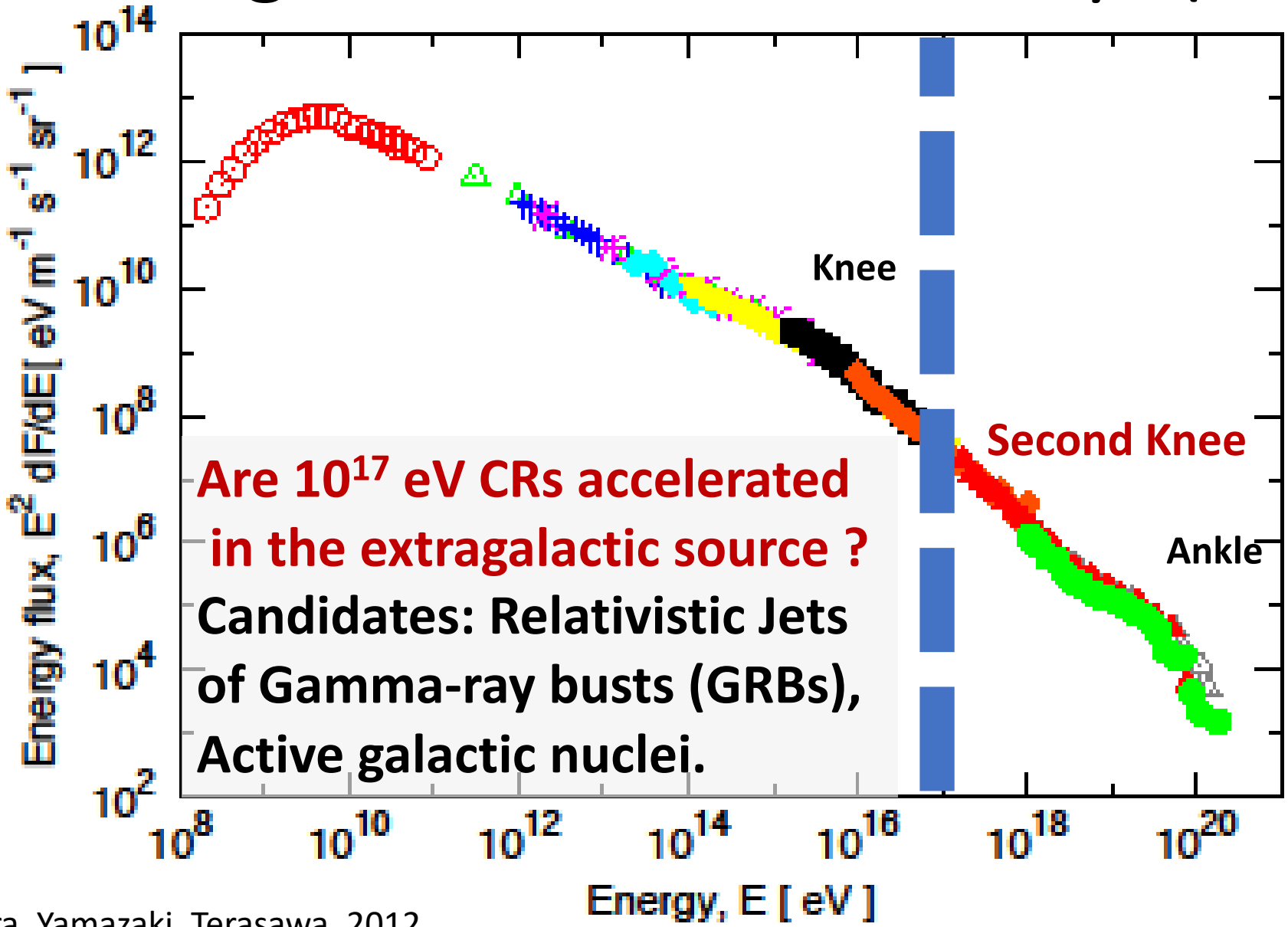

Are 10^{17} eV CRs accelerated in the extragalactic source ?

Candidates: Relativistic Jets of Gamma-ray busts (GRBs), Active galactic nuclei.

Ohira, Yamazaki, Terasawa, 2012

The relativistic jet interacts with interstellar medium (ISM) or circum-stellar medium (CSM).

→ Relativistic collisionless shocks mediated by the Weibel instability

- **occurs in an anisotropic temperature plasma.**
- **is a possible generation process of magnetic fields.**

Spitkovsky et al. 2008

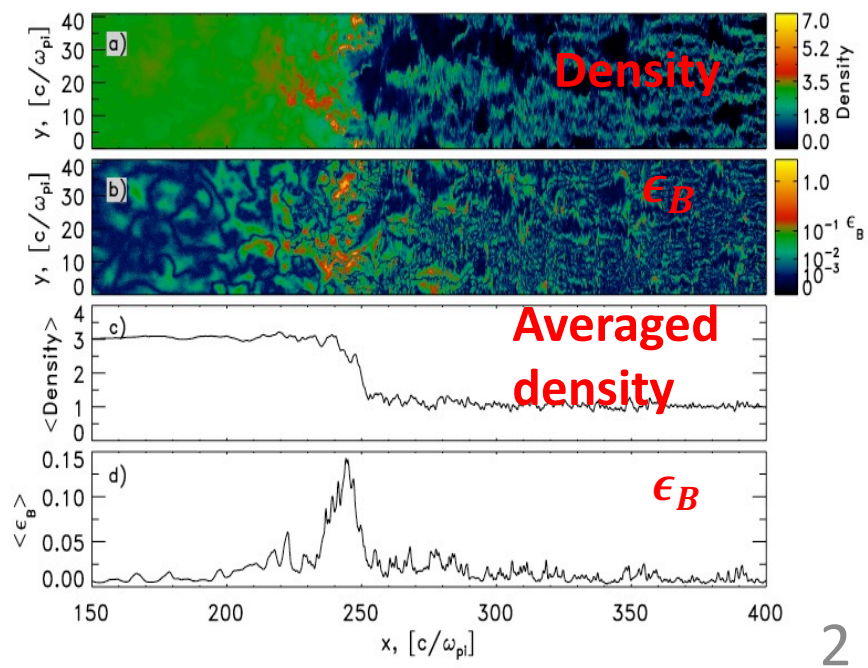

PIC simulations of the Weibel mediated shocks :

The Weibel magnetic field has Strong small-scale fluctuation.

$$\mathbf{r}_{\mathrm{g}} \gg \lambda_{\delta_{\mathrm{B}}}$$

Particle acceleration in the Weibel-mediated shocks:

For $\mathbf{r_g} \gg \lambda_{\delta_B}$, the diffusion efficient : $\mathbf{D(E_p) = c\lambda_{\delta B}\left(\frac{E_p}{eB\lambda_{\delta B}}\right)^2}$

Shalchi & Dosch 2009; Plotnikov et al. 2011, 2013

Then, $\frac{\gamma_{max}}{\gamma_0} \sim (2\epsilon_B \lambda_{\delta_B} \omega_{pp} t)^{1/2}$.

$\lambda_{\delta B}$: coherent length of δB

$\varepsilon_B \sim \frac{B^2/8\pi}{\Gamma_{sh}^2 n_{ISM} mc^2}$, ω_p: plasma frequency

At $\mathbf{t = t_{age} \sim (R_{dec}/c)/\Gamma_{sh}}$,

Deceleration radius of the shock, $\mathbf{R_{dec} \sim 10^{17} E_{exp,54}^{1/3} n_{ISM,0}^{-1/3} \Gamma_{sh,2}^{-2/3} cm}$

$\epsilon_{B,-3}\lambda_{c/\omega_{pp}} \sim 0.03$ **(from PIC simulation)**

The maximum Lorentz factor becomes

$$\gamma_{max,p} \approx 10^8 E_{exp,54}^{3/4} n_{ISM,0}^{-1/2} R_{dec,17}$$ **In ISM frame**

$$E_{max,p} \approx 10^{17} eV$$

if the b-fields is constant in the far downstream region.

However, the Weibel generated b-field rapidly decays.

$\lambda_{\delta B} \ll r_g$ is inefficient for particle acceleration.

Purpose of our study

Previous studies :

Nonlinear evolution of the Weibel instability for shocks in uniform plasmas → B-fields rapidly decay.

However, there must be some density fluctuations in the ISM or CSM.

Armstrong et al. 1995, Chugai & Danzieger 1994, Smith et al. 2009, Yalinewich & Zwart 2019
Drury & Falle 1986, Ohira 2013, 2014, 2016

In this study :

We investigate the magnetic field amplification in the downstream region of the relativistic collissionless shock propagating to the inhomogeneous ISM, by using two-dimensional PIC simulations.

Simulation Set Up

- **Two-dimensional electromagnetic PIC code (pCANS)**
- **X-Y plane with periodic boundary condition in the y-direction.**
- **Box Size:** $L_x = 1.2\times10^4\ {}^{c}/_{\omega_p}$, $L_y = 86\ {}^{c}/_{\omega_p}$, **Cell Size: ΔX=ΔY=0.1**${}^{c}/_{\omega_p}$
- **Unmagnetized** $e^{\pm}$ **plasmas (**$n_{e^+} = n_{e^-}$**) with Lorentz factor Γ = 10,**v_{th}**=0.1c.**
- **Initial spatial distribution of** $e^{\pm}$**:**

$$n(x,y) = n_0\{1 + 0.5\sin(2\pi kx/L_x)\}$$

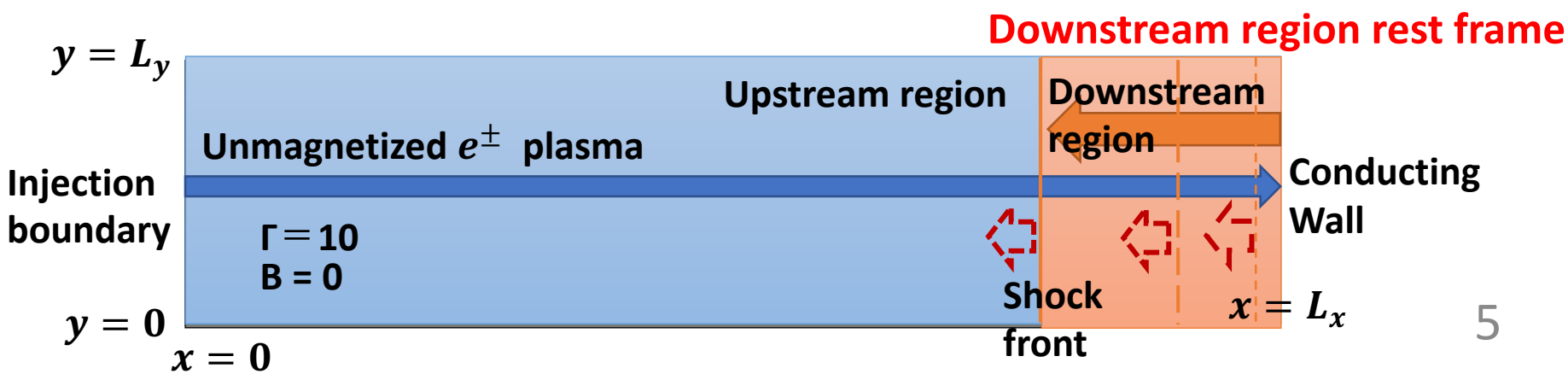

Simulation Set Up

- **Two-dimensional electromagnetic PIC code (pCANS)**
- **X-Y plane with periodic boundary condition in the y-direction.**
- **Box Size:** $L_x = 1.2\times10^4\ {}^{c}/_{\omega_p}$, $L_y = 86\ {}^{c}/_{\omega_p}$, **Cell Size: ΔX=ΔY=0.1**${}^{c}/_{\omega_p}$
- **Unmagnetized** $e^{\pm}$ **plasmas (**$n_{e^+} = n_{e^-}$**) with Lorentz factor Γ = 10,**v_{th}**=0.1c.**
- **Initial spatial distribution of** $e^{\pm}$:

$$n(x,y) = n_0\{1 + 0.5\sin(2\pi k x/L_x)\}$$

$$k = 10$$

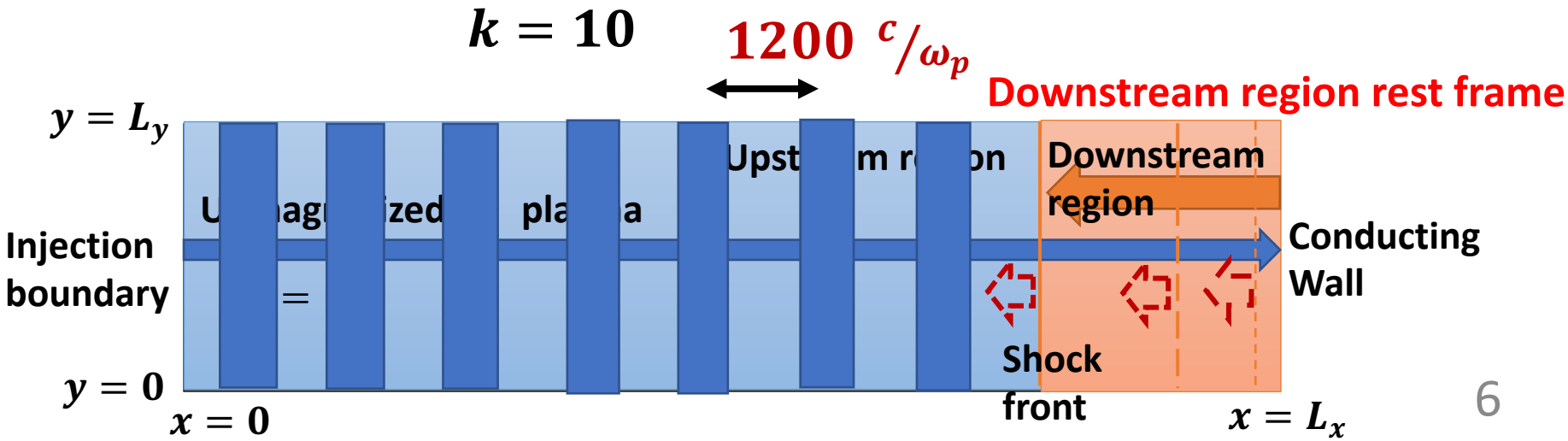

Uniform
(at $t\omega_{pe} = 5000$)

No-uniform
(shock in the $\frac{n_0+\delta n}{n_0} = 1.5$ region) at $t\omega_{pe} = 4800$

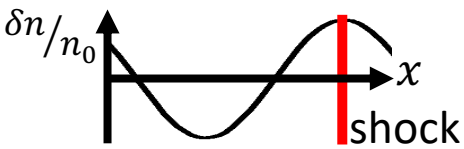

No-uniform
(shock in the $\frac{n_0+\delta n}{n_0} = 0.5$ region) at $t\omega_{pe} = 5200$

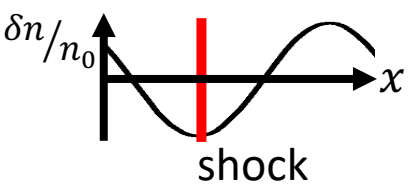

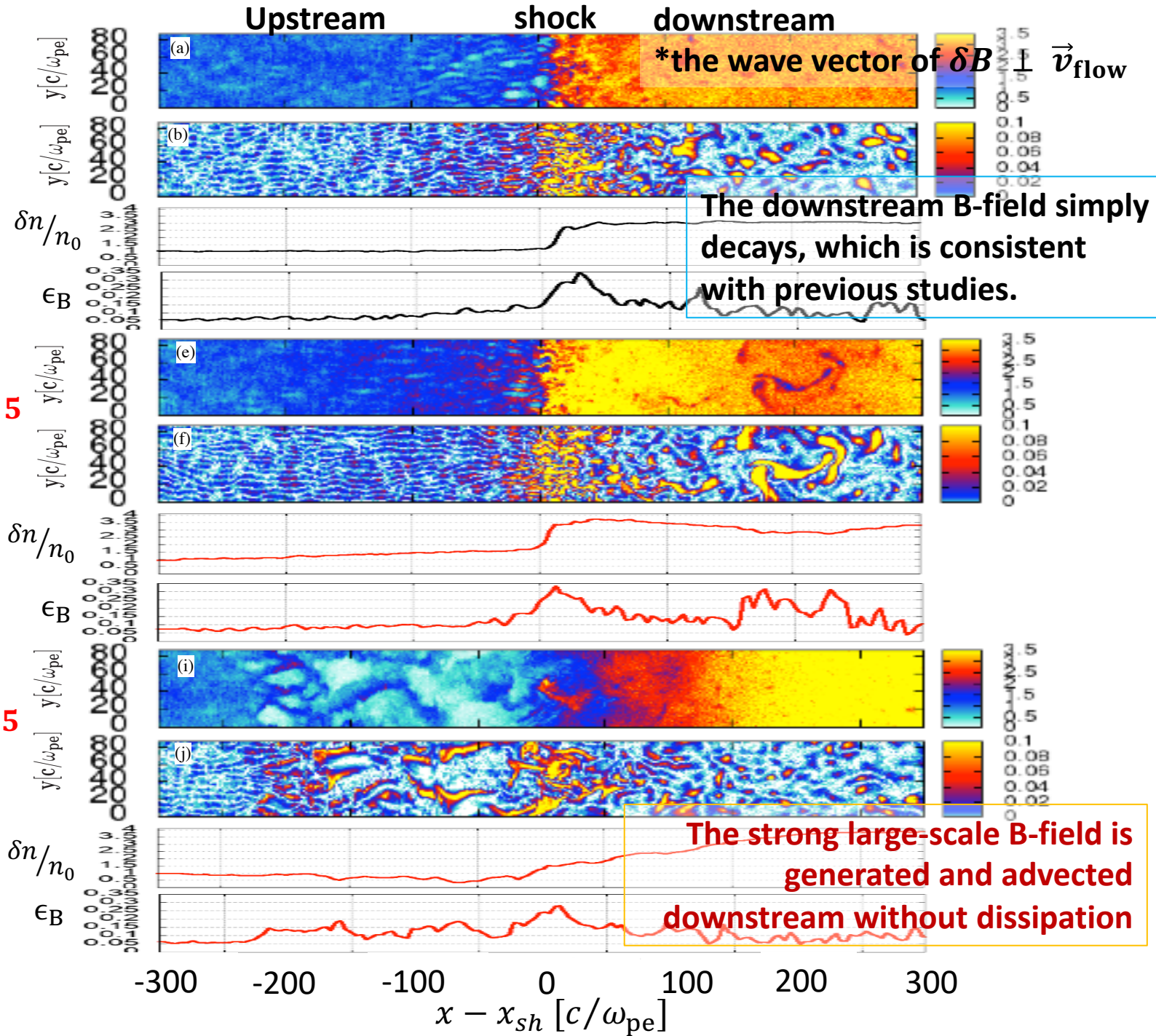

The downstream B-field simply decays, which is consistent with previous studies.

The strong large-scale B-field is generated and advected downstream without dissipation

The spatial evolution of the transversely averaged ε_B in the downstream region at the later time $(t = 6100\omega_p^{-1})$

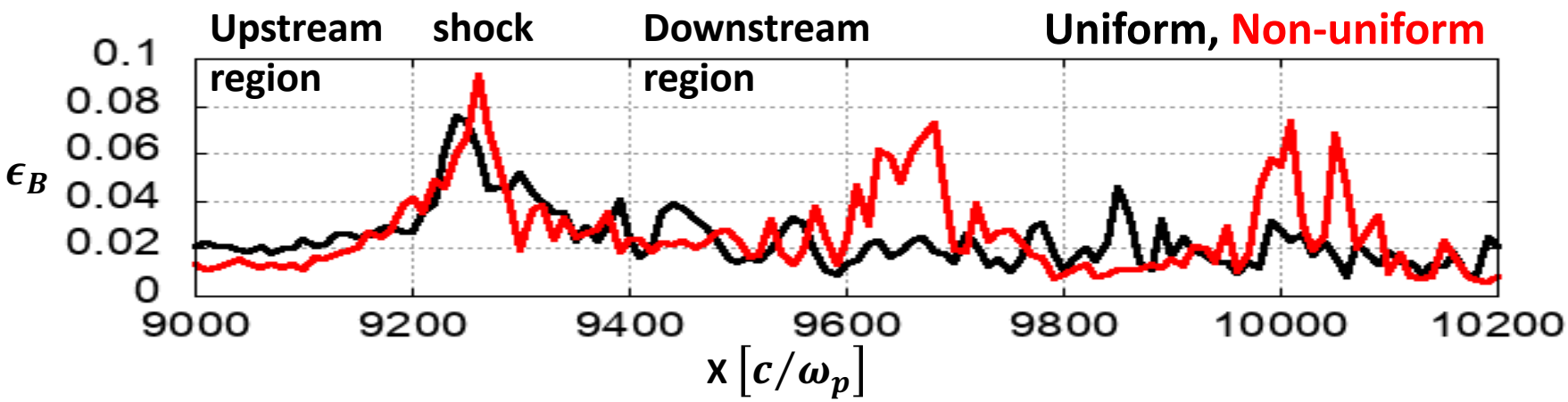

Uniform:

The magnetic field simply decays.

Non-uniform:

The magnetic field decays much slower than uniform case. Two peaks of ϵ_B were generated when the shock was passing through the low-density region.

The inhomogeneity of the upstream density is crucial in the generation of the downstream magnetic field.

$L_x \times L_y = 1.2 \times 10^4 \times 86\ {}^{c}/_{\omega_p}$

Density & velocity in the x-direction $(t = 6100\omega_p^{-1})$

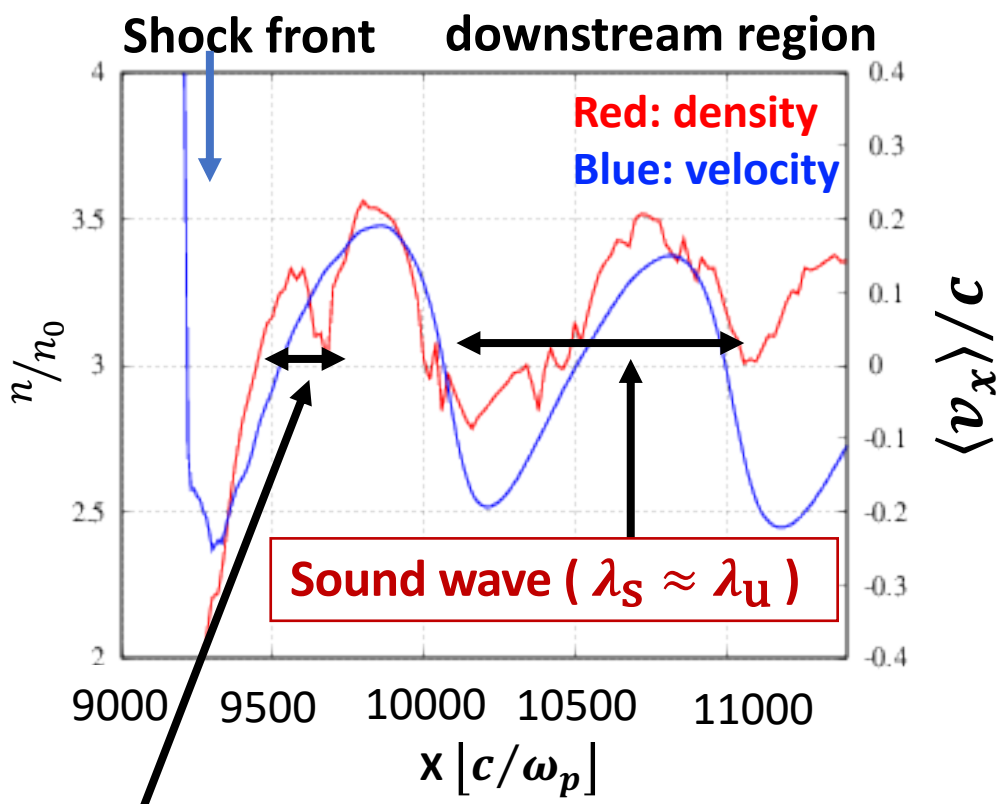

λ_e:wavelength of the entropy wave
λ_s: wavelength of the sound wave
λ_u:wavelength of the upstream incoming wave

Sound waves and entropy waves are generated as expected by hydrodynamic analysis of the shock-wave interaction.

Each wavelength is consistent with result from the linear analysis for the shock front.

The sound wave might play crucial role on the particle acceleration!

Summary arXiv: 1907.08939

We have investigated the evolution of b-field in the downstream region of relativistic collisionless shocks propagating into inhomogeneous media.

- ✓ **A larger-scale magnetic field is generated in the shock precursor region and hardly decay after it is advected downstream.**
- ✓ **The sound and entropy waves are generated in the downstream region. The sound wave could be crucial for the particle acceleration. (These waves potentially generate temperature anisotropy)**
- ✓ **Inhomogeneous upstream density significantly affects the postshock region of collisionless shocks, even if the wavelength of the upstream inhomogeneity is much larger than the kinetic scale.**

The energy spectra in the downstream region

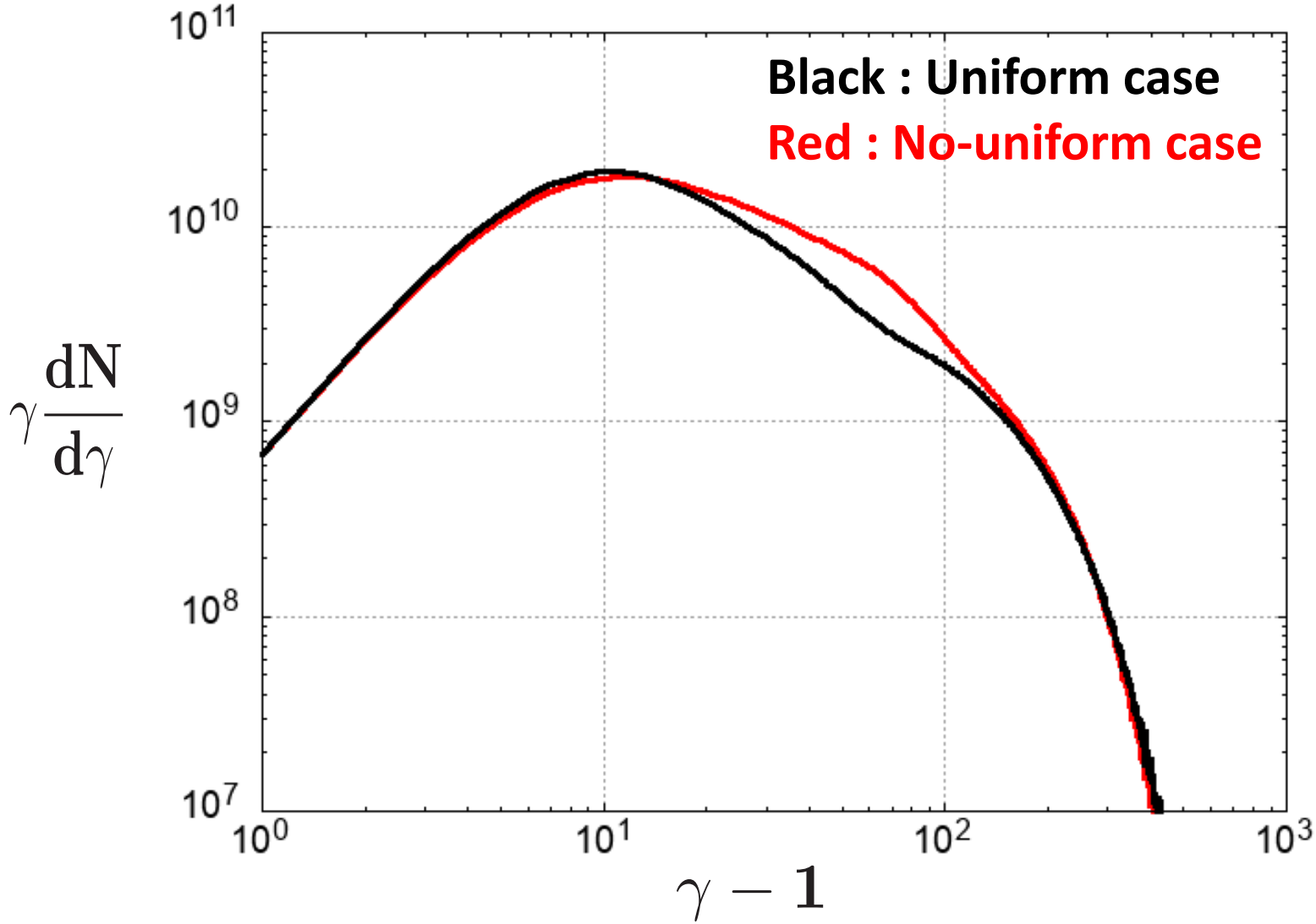

$L_x \times L_y = 1.2 \times 10^4 \times 86\ {}^{c}/_{\omega_p}$

Density & velocity in the x-direction $(t = 6100\omega_p^{-1})$

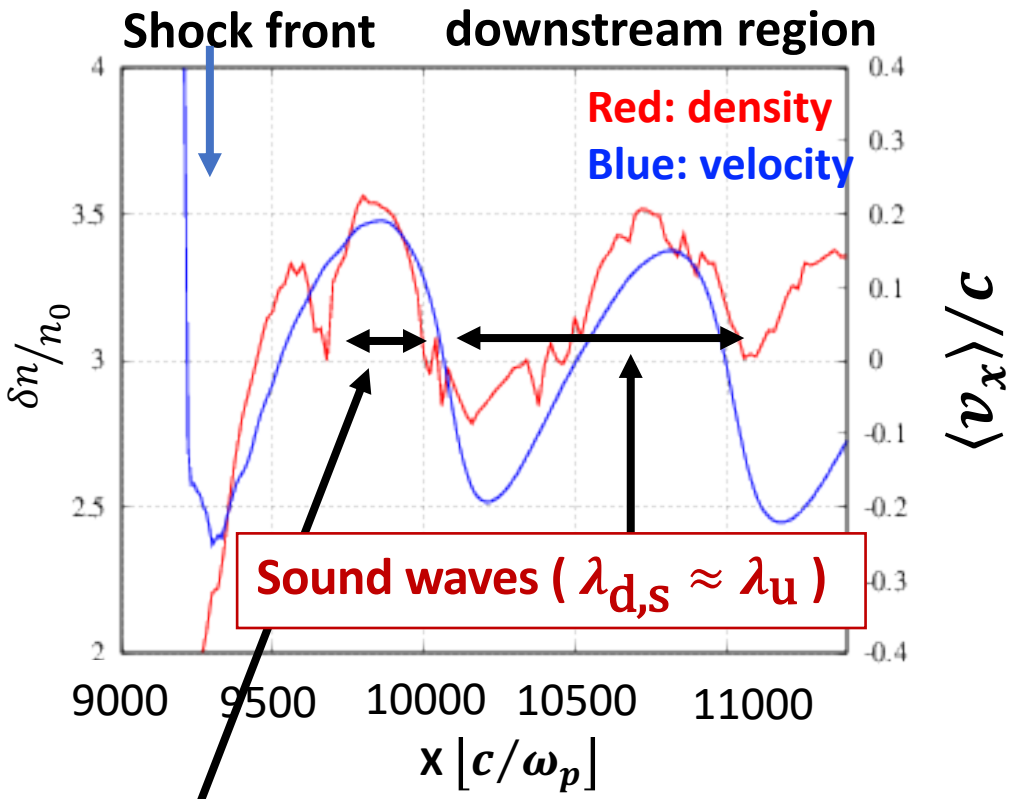

Entropy waves ($\lambda_{d,e} \approx \frac{1}{3}\lambda_u$)

Sound waves and entropy waves do not decay during the simulation time.

$$\tau_{\text{decay}} \equiv \frac{1}{3} r_g c,$$

$$\tau_{\text{decay}} = \frac{\lambda_s^2}{\kappa}$$

$$= \begin{cases} 10^6\ \omega_{\text{pe}}^{-1} \left(\frac{\gamma}{10}\right)^{-1} \left(\frac{\Gamma}{10}\right) \left(\frac{\epsilon_B}{10^{-2}}\right)^{\frac{1}{2}} \left(\frac{\lambda_{\delta\rho}}{1.2\times10^3 c/\omega_{\text{pe}}}\right)^2 \\ 10^5\ \omega_{\text{pe}}^{-1} \left(\frac{\gamma}{10}\right)^{-1} \left(\frac{\Gamma}{10}\right) \left(\frac{\epsilon_B}{10^{-2}}\right)^{\frac{1}{2}} \left(\frac{\lambda_{\delta\rho}}{4.0\times10^2 c/\omega_{\text{pe}}}\right)^2 \end{cases}$$

The spatial profile of the velocity & Temperature anisotropy

$(t = 6100\omega_p^{-1})$

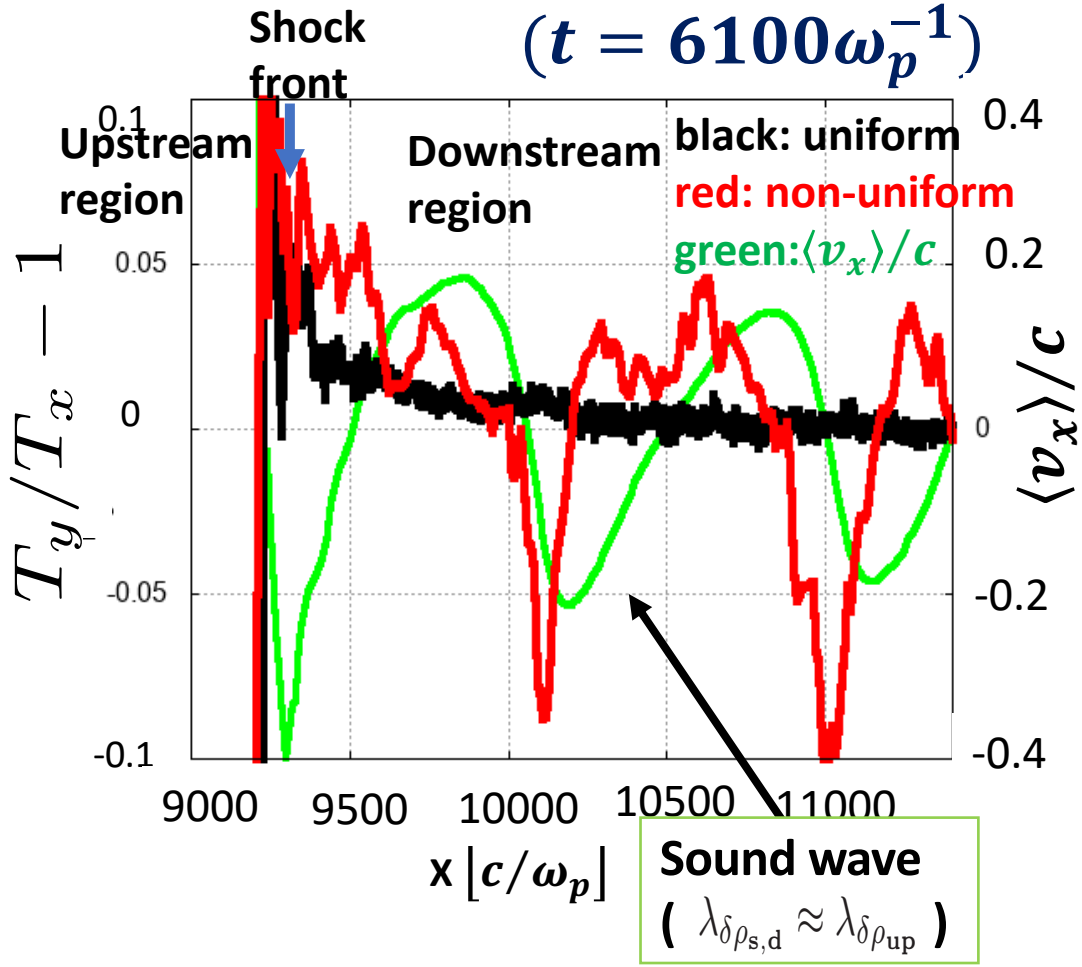

$$\frac{T_{x,y}}{mc^2} = \int_{p_{min}}^{p_{max}} d^3p \frac{p_{x,y}^2}{\gamma m^2 c^2} f(p_x,\ p_y,\ p_z)$$

given by Yoon, 2007 **in local plasma rest frame**

Sound wave propagating to the downstream direction is produced.

Temperature anisotropy:
is almost 0 (uniform case),
oscillates synchronously with the sound wave (non-uniform case)
Average amplitude is 0.05.

$T_y < T_x$ in $\nabla\beta_x < 0$:
the steepening of the sound wave and diffusion of high-energy particles.
$T_y > T_x$ in the other regions :
diffusion of high-energy particles.

The growth rate of the Weibel instability

$$\gamma_{max} = \frac{2}{3\sqrt{3}} \frac{T_x}{mc^2} \left(\frac{T_y}{T_x} - 1 \right)^{3/2} \omega_{pe}$$

given by Yoon, 2007

→ $t_{max} \sim \text{a few} \times 10^2 \left(\frac{T_y/T_x - 1}{0.05} \right)^{-3/2} \omega_{pe}^{-1}$ for $k_{max} = \frac{1}{\sqrt{3}} \frac{\omega_{pe}}{c}$

The oscillation period of the temperature anisotropy

→ $t_{osc} \sim 10^2 - 10^3 \omega_{pe}^{-1}$ **Comparable…**

If the free energy of the temperature anisotropy is fully converted to the magnetic field energy,

$$|Ty/T_x - 1| \times U_{th} \xrightarrow{\text{Weibel instability}} U_B$$

$$\epsilon_B \sim |Ty/T_x - 1| \sim 5 \times 10^{-2} \gg 10^{-5}$$

(Estimate from the observation of the afterglow)

We could see the generated b-fields in the far downstream region, if the magnetic field generated in the shock front sufficiently decays.

The Origin of the Temperature Anisotropy

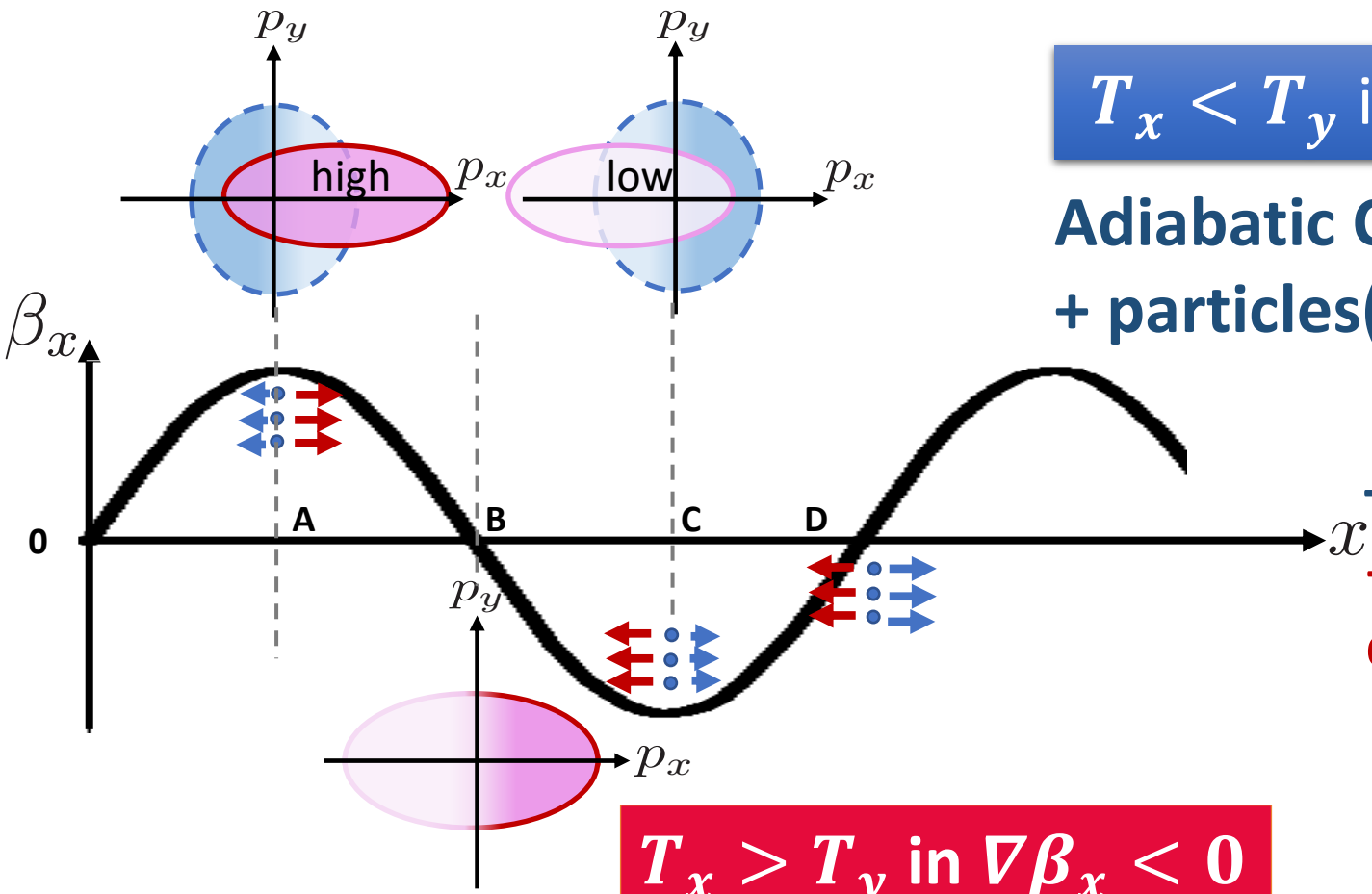

$T_x < T_y$ in $\nabla\rho > 0$

Adiabatic Compression
+ particles($P_y < P_x$) diffusion

- - local (A,C) rest frame
– the region B, downstream rest frame

$T_x > T_y$ in $\nabla\beta_x < 0$

High energy ($P_y < P_x$) particle escaping from A, C

Generation of a Temperature Anisotropy

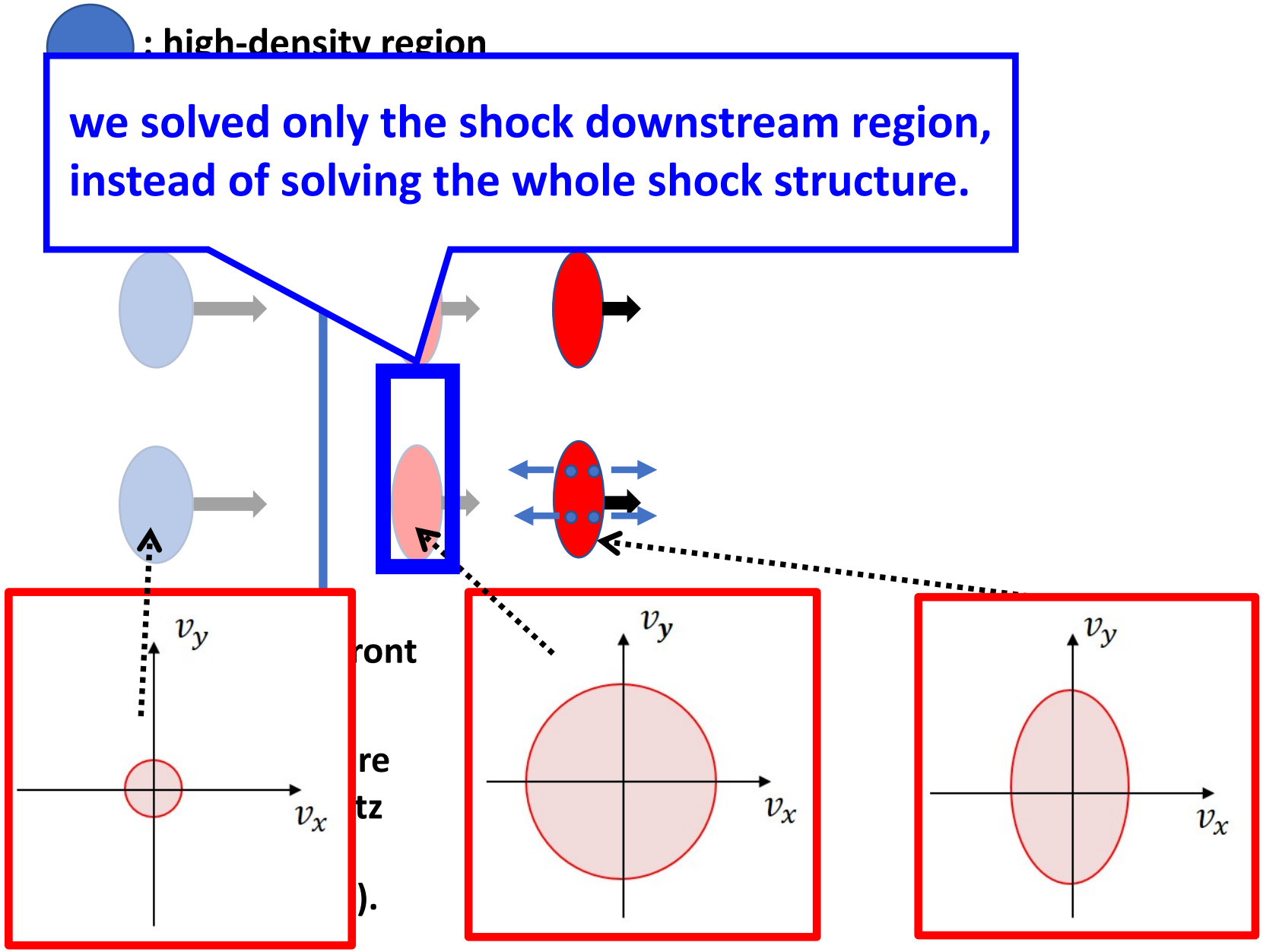

Simulation Set up

2D electromagnetic particle in cell code (pCANS)

- **Unmagnetized $e^{\pm}$ plasmas**

  B$= 0, n_{e^+} = n_{e^-}$

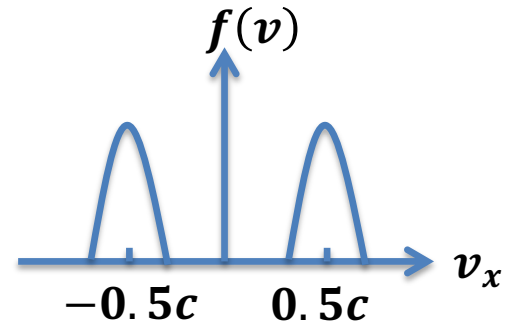

- **Two counter-streaming beams in the x direction**

  Drift velocity $v_d = \pm 0.5c$

  Thermal velocity $v_{th} = 0.1c$

- **Spatial distribution of the $e^{\pm}$**

  $$n(x, y) = n_0\{1 + 0.5 \sin 2\pi y / L_y\}$$

  $n_0 = 40$ /cell/species

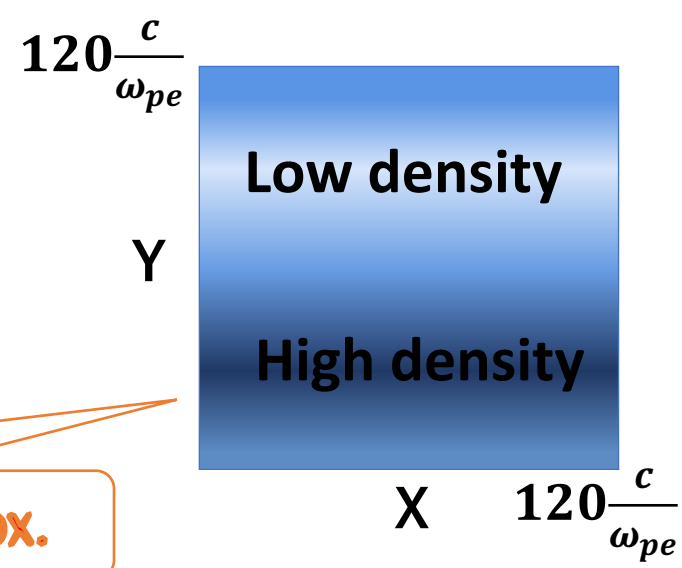

there is one wavelength in the simulation box.

Generation of a Temperature Anisotropy

we solved only the shock downstream region, instead of solving the whole shock structure.

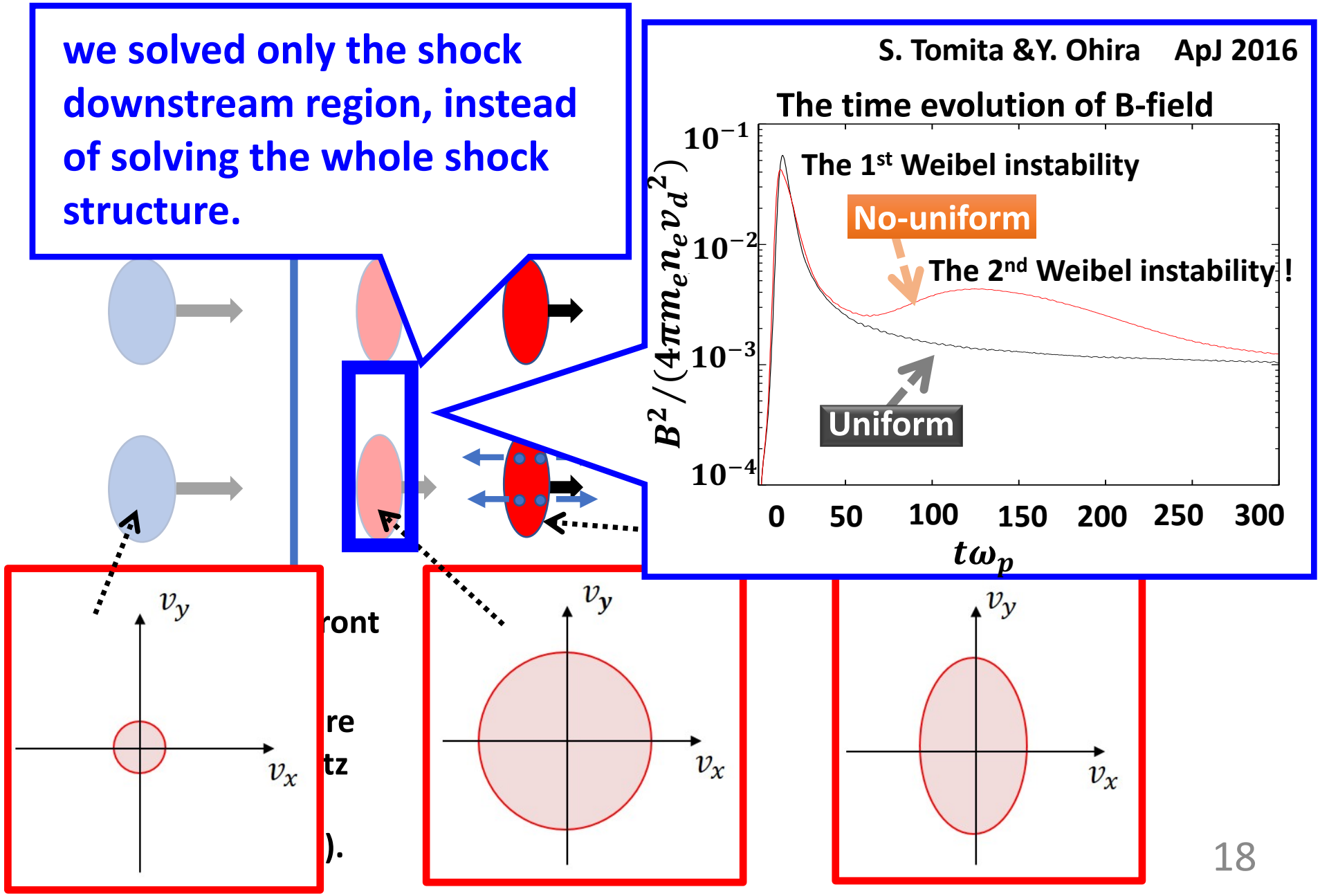

Time evolution of the temperature anisotropy

$(L_y = 240\, c/\omega_p)$

After the 1st saturation, A increases.
∵particles moving to the y-direction escape to the low density region, so that the temperature in the y-direction decreases.

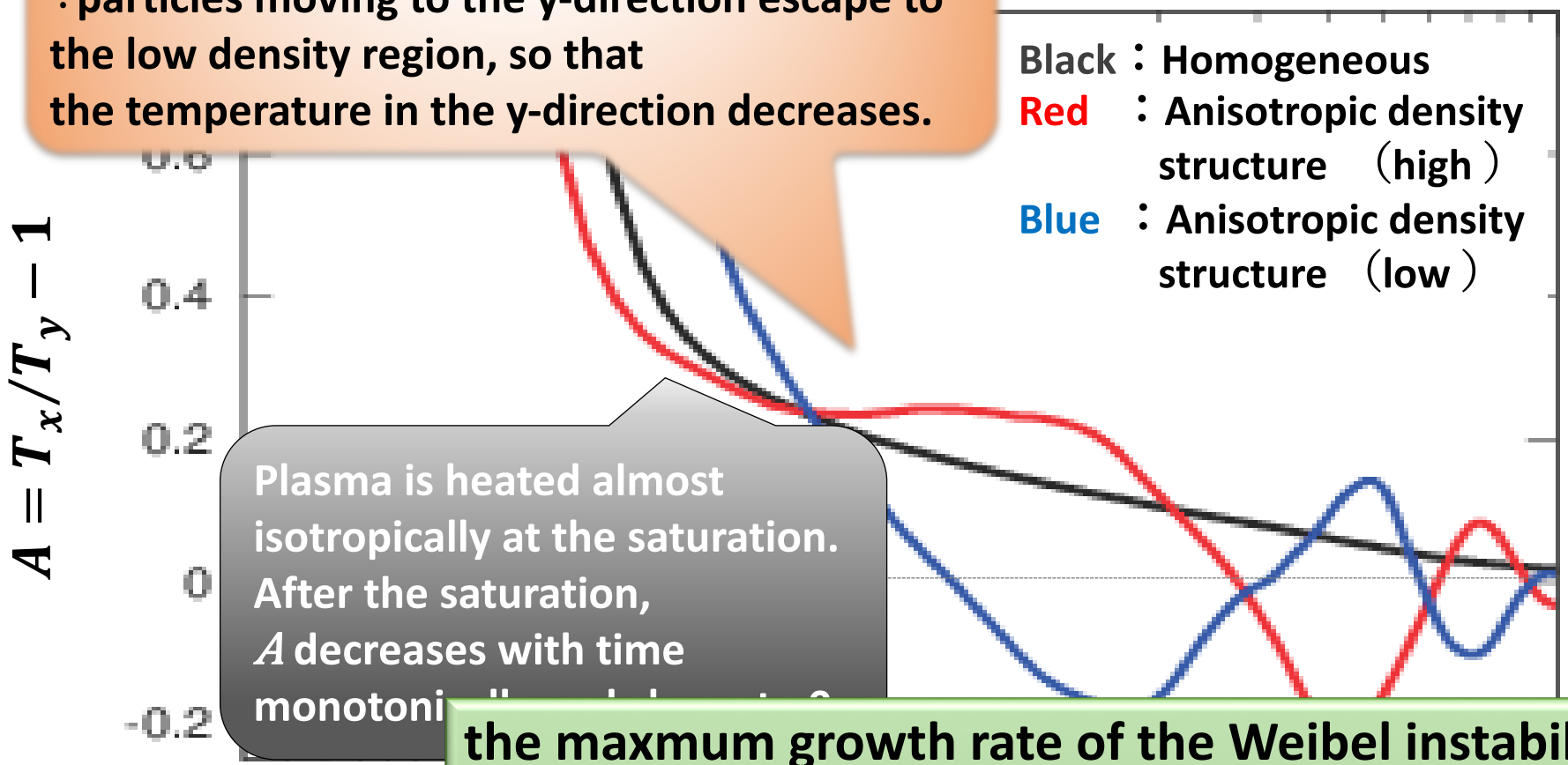

Plasma is heated almost isotropically at the saturation.
After the saturation, A decreases with time monotoni

the 1st sa

the maxmum growth rate of the Weibel instability
$\gamma_{max} \approx 1.6\times10^{-2}\,\omega_p$ ($k_y \approx 0.26\,\omega_p/c$)
→consistent with our simulation.
The 2nd generation of magnetic fields is also due to the Weibel instability.

The length dependence of the magnetic field generation

Black：Homogeneous

Green: Anisotrpic density structure $(L_y = 120c\omega_p^{-1})$

Red ： Anisotrpic density structure $(L_y = 240c\omega_p^{-1})$

Blue ： Anisotrpic density structure $(L_y = 480c\omega_p^{-1})$

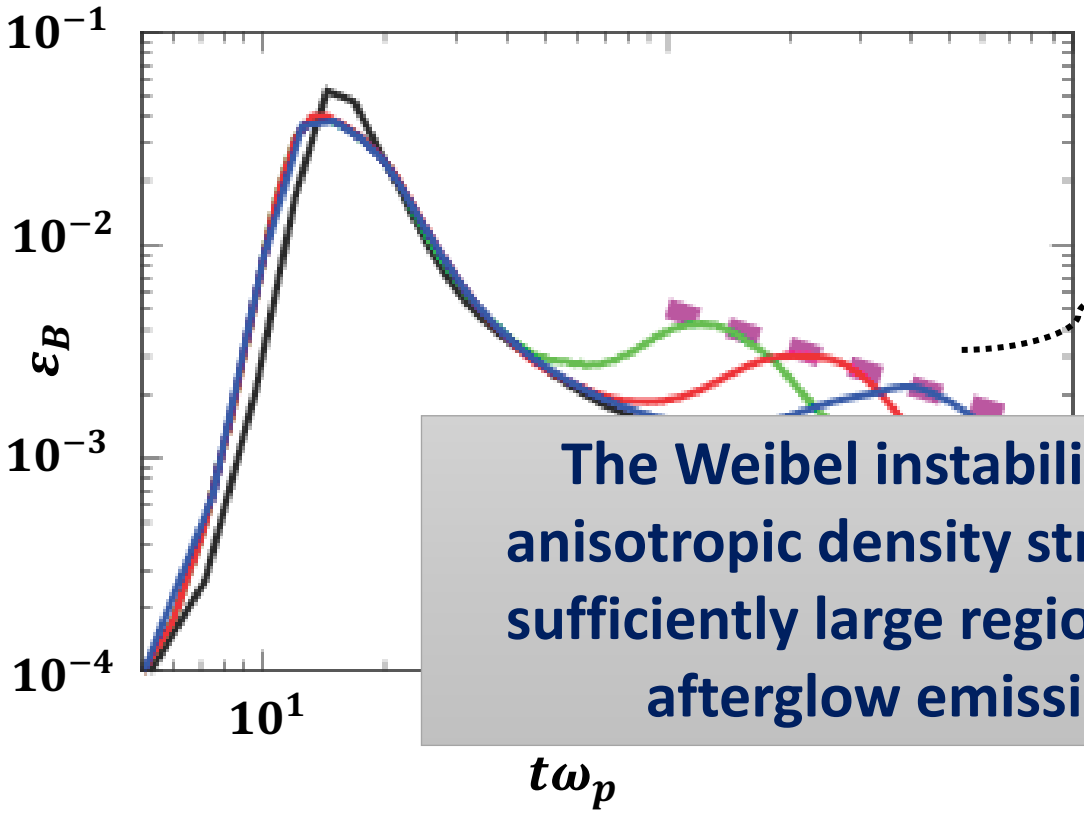

The timescale of the 2nd generation of magnetic fields

II

The sound crossing time of the high density structure.

Scaling

$$\varepsilon_B \approx 0.08\times(t\omega_p)^{-0.6}$$

If the lengthscale of a density

c/ω_p

$\sim 10^7\omega_p^{-1}$

$^{-8} - 10^{-3}$

$t_{rad}\sim 10^{\ } - 10^{\ }\omega_p^{-1}$

The Weibel instability driven by an anisotropic density structure can cover sufficiently large regions to explain the afterglow emission of GRBs!